

Experiment and simulations on the energy reservoir effect in femtosecond light filaments

W. Liu

Centre d'Optique, Photonique et Laser (COPL) and Département de Physique, de Génie Physique et d'Optique, Université Laval, Québec, Québec G1K 7P4, Canada, and Max-Planck-Institut für Physik komplexer Systeme, Nöthnitzer Strasse 38, D-01187 Dresden, Germany

F. Théberge

Centre d'Optique, Photonique et Laser (COPL) and Département de Physique, de Génie Physique et d'Optique, Université Laval, Québec, Québec G1K 7P4, Canada

E. Arévalo

Max-Planck-Institut für Physik komplexer Systeme, Nöthnitzer Strasse 38, D-01187 Dresden, Germany

J.-F. Gravel

Centre d'Optique, Photonique et Laser (COPL), and Département de Physique, de Génie Physique et d'Optique, Université Laval, Québec, Québec G1K 7P4, Canada

A. Becker

Max-Planck-Institut für Physik komplexer Systeme, Nöthnitzer Strasse 38, D-01187 Dresden, Germany

S. L. Chin

Centre d'Optique, Photonique et Laser (COPL), and Département de Physique, de Génie Physique et d'Optique, Université Laval, Québec, Québec G1K 7P4, Canada

Received March 30, 2005; revised manuscript received May 23, 2005; accepted June 11, 2005

We report the results of an experiment and numerical simulations that demonstrate the large spatial extent and the effect of the so-called energy reservoir during the filamentation of femtosecond laser pulses in air. By inserting pinholes of different sizes in the filament path we observe different stages of development ranging from the termination of the filament, through its partial survival, to undisturbed propagation. A background containing up to 50% of the pulse energy is found to be necessary to maintain the filament formation, including a first refocusing. © 2005 Optical Society of America

OCIS codes: 190.5530, 260.5950, 320.2250, 320.7110.

Filament formation of high-power femtosecond laser pulses in air has attracted much interest since its first observation about a decade ago,¹ due mainly to its promising applications in atmospheric remote sensing² and lightning control.^{3,4} The dynamics of filamentation is nowadays understood as based on a subtle interplay among the optical Kerr effect, the defocusing effect of the self-generated plasma, and several smaller effects. Recently, the role of the low-intensity background of the pulse for the filament formation, which embraces the tiny high-intensity inner filament core, has become a center of interest. Its existence was noticed already in the first demonstrations of filamentation in air^{1,5,6} and was first interpreted in computer simulations as a background energy reservoir of the filament core.⁷ Several experiments⁶⁻⁹ provided further support for this interpretation. Recently, it was further shown in an experiment¹⁰ and subsequent numerical simulations^{8,11,12} that filaments are robust after a collision with a water droplet. This observation has been attributed as due to an energy transfer from the background to the filament core. Also, results of a variational analysis¹³ indicate that the process of

self-focusing is already strongly influenced by the wide background of the pulse.

Although previous experimental and theoretical work provides evidence for the crucial role of the background energy reservoir for the formation of the filament, the size of the reservoir and the portion of the pulse energy located in the background are undetermined. Knowledge of these parameters would provide insight into over which transverse dimension the pulse has to be controlled to reach long filaments. In this Letter we show that the size of the reservoir is about 5–10 times larger than the high-intensity core and contains up to 50% of the pulse energy, in agreement with recent theoretical predictions.¹² Our conclusions are based on the results of an experiment in which pinholes of diameters between 220 μm and 2 mm are used to block the background reservoir and the results of numerical simulations, which indicate that diffraction of energy at the edges of the background has a strong effect on the long-scale evolution of the filament core.

The commercial chirped-pulse amplification femtosecond Ti:sapphire laser system (Spectra Physics)

used in the experiment has been described in detail elsewhere.^{9,14} The laser beam used in this work had the following characteristics: 800 nm, 40 fs, 10 Hz, 2.5 mJ/pulse. The peak power is more than 10 times higher than the critical power for self-focusing in air¹⁴ (~6 GW). The initial beam diameter was reduced to 2 mm (FWHM) by an inverse telescope, and a single filament was obtained in air.

Pinholes of different diameters (220 μm to 2 mm, thickness between 35 and 60 μm) were introduced coaxially to the propagation axis of the beam. The evolution of the filament formation was observed by using an intensified CCD camera (ICCD, Princeton Instruments, PI-MAX 512) to image the fluorescence emitted from the nitrogen molecule (N_2) and nitrogen ion (N_2^+) in the filament core.¹⁵ The ICCD camera was installed perpendicularly to the pulse propagation axis, and the fluorescence signal was collected and imaged onto the ICCD detector by using a single fused silica plano-convex lens ($f=63$ mm, diameter 38.1 mm). A bandpass filter (1 mm thick UG11, Corion) together with a 0° incident 800 nm dielectric mirror were placed in front of the camera to integrate the light emission over the strongest N_2 and N_2^+ bands around 350 nm while rejecting the scattered light from the pump laser. There is a good overlap between the bandpass filter transmission curve and the strongest N_2 and N_2^+ bands around 350 nm.¹⁶ With this configuration, a length of about 0.5 m along the laser propagation axis was covered by the field of view of the ICCD detection system. A slim black screen (~3 cm wide) was put beside the pinhole to avoid strong scattering of the laser light from the metal surface of the pinhole to the detector.

Images acquired by the ICCD camera are shown in Figs. 1(a)–1(e). Each image results from an accumulation of 1000 laser shots. The propagation distance is scaled with respect to the output lens of the telescope. Figure 1(a) represents the free propagation of the pulse (without pinhole); a bright line as long as almost half a meter is seen along the propagation axis. The onset of the filament is located near the left-hand side of the image. The other panels on the left-hand side of Fig. 1 show the images for pinholes of different diameters inserted at 1.73 m, starting

with a diameter of 220 μm [Fig. 1(b)] to as great as 2 mm [Fig. 1(e)]. The black gap between 1.7 and 1.8 m in these four panels is due to the black screen. It is seen that for the smallest diameter [Fig. 1(b), 220 μm] the plasma column is terminated by the pinhole. In this case, no significant damage of the pinhole was found after the experiment, which indicates the high stability of the laser system and ensures the success of our experiments. As the diameter of the pinhole is doubled [Fig. 1(c), 440 μm] the filament partially survives out to about 1.9 m. Here, the filament appears to be stronger than for free propagation, which we attribute [as the white spot in Fig. 1(b)] to a geometrical focusing, near-field diffraction induced by the small pinholes. When the pinhole diameter is increased to 1 mm [Fig. 1(d)] and 2 mm [Fig. 1(e)], the filament formation looks unchanged compared with the case of free propagation within the field of view of the camera.

To provide further insight, we have performed numerical simulations of the amplitude envelope A based on the nonlinear wave equation written in the retarded coordinate system (using the slowly varying envelope approximation):

$$2ik_0 \frac{\partial A}{\partial z} = \Delta_{\perp} A - k_2 k_0 \frac{\partial^2 A}{\partial t^2} + 2 \frac{k_0^2}{n_0} (\Delta n_{\text{Kerr}} + \Delta n_{\text{plasma}}) A - ik\alpha A. \quad (1)$$

In Eq. (1) diffraction, dispersion, and the Kerr effect as well as plasma generation and energy losses due to multiphoton and tunnel ionization are considered. Values for k_0 , k_2 , Δn_{Kerr} , Δn_{plasma} and α are adapted from Ref. 14, and parameters of the present laser system (2.5 mJ, 40 fs, 2 mm diameter at FWHM) have been used as initial conditions in the simulations. The effects of the pinholes are simulated by applying an energy transmission function at 1.7 m. The transmission function is set to be unity from the axis to the corresponding pinhole radius and smoothed toward the outer edge by a Gaussian function with 10 μm ($1/e^2$) width. The pinholes are treated as hard apertures; thickness is found to play a minor factor.

Electron density distributions [Figs. 1(f)–1(j)] agree well with the experiments; each panel corresponds to the experimental result on the same row. Also, for the percentage of initial energy transmitted through the pinhole [Fig. 2(a)] there is good agreement between the experimental results (open triangles, measured by a powermeter 1.5 m after the pinhole) and those from simulations (solid squares) for all pinhole diameters. The results for the on-axis electron density distribution from numerical simulation, shown in Fig. 2(b), reveal that the refocusing peak, which appears roughly between 2.2 and 3 m for free propagation (solid curve), is suppressed for the smaller pinhole (1 mm, dashed curve) but not for the pinhole of 2 mm diameter (dotted curve). Thus a background, whose transverse dimension is about 5–10 times as large as the filament core and which contains up to 50% of the pulse energy [see Fig. 2(a)], has to propagate together with the filament core in order to maintain the full length of the filament, including one refocusing.

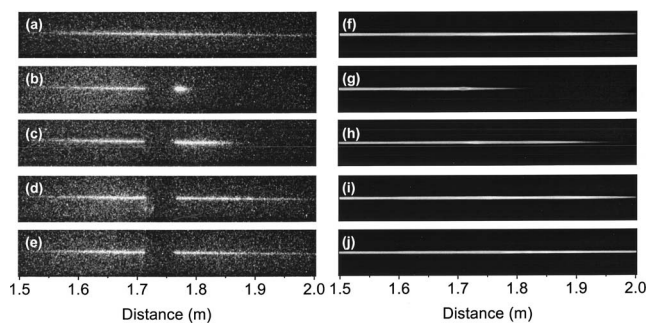


Fig. 1. Left column, images of the nitrogen fluorescence signal recorded by an ICCD camera. Right column, electron density distribution from numerical simulations. (a), (f) Free propagation; (b), (g) pinhole diameter 220 μm ; (c), (h) pinhole diameter 440 μm ; (d), (i) pinhole diameter 1 mm; (e), (j) pinhole diameter 2 mm.

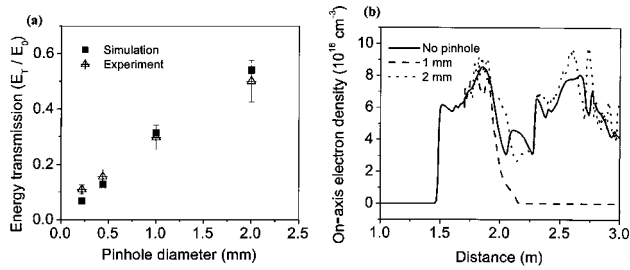


Fig. 2. (a) Energy transmission through the pinhole; (b) On-axis electron density distribution from numerical simulations.

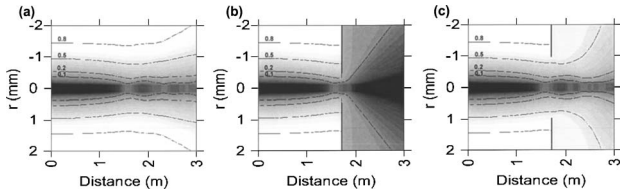


Fig. 3. Results of numerical simulations for the radial energy distribution as a function of propagation distance: (a) free propagation, (b) pinhole diameter 1 mm, (c) pinhole diameter 2 mm.

Numerical results for the energy distributions in Fig. 3 suggest that a diffraction of energy at the edges of the background leads to a leakage of energy, which results in a termination of the filament. Gray levels represent the energy percentage within a given radius r_0 about the propagation axis: the lighter the color, the larger the portion of energy enclosed. Four contour lines, indicating the 10%, 20%, 50%, and 80% levels, are plotted to guide the eye. The oscillations of the inner contour lines indicate the energy exchange between the filament core and the outer background [see Fig. 3(a) for the case of free propagation]. The pinholes initiate a diffraction at the edges of the background at an earlier stage of the filament formation compared with the case of free propagation [see Figs. 3(b) and 3(c) for 1 mm and 2 mm pinholes, respectively]. For the smaller pinhole this results in the termination of the filament before refocusing takes place.

The above results have important implications for long-range filament formation. It is obvious that for the maintenance of the high-intensity filament core, which contains only about 10% of the pulse energy,⁶ the propagation of a wide background, in which 50% or more of the pulse energy is located, together with the core is needed. For the filament formation it is obviously more critical to avoid a diffraction of energy at the edges of the background than a collision with a (small) droplet near the center. Our results clearly rule out any self-guiding model for the filament core but do favor the moving focus⁶ and spatial replenishment⁷ models. They may, however, raise the question of whether the whole structure, i.e., core and background, should not be called the filament and whether it could be described by spatial soliton solutions or a superposition of such solutions.^{8,12}

In conclusion, our results verify that the formation of robust filaments is due to the wide low-intensity background around the tiny high-intensity core. We have shown that this background is more than 5 times larger than the filament core and contains up to 50% of the pulse energy. The robustness of the filament formation does depend crucially on diffraction of energy at the edges of the weak background.

This work was partially supported by the Natural Sciences and Engineering Research Council, Defence Research and Development Canada, Canada Research Chairs, the Canadian Institute for Photonic Innovations, the Canada Foundation for Innovation, FemtoTech, and Le Fonds québécois de la recherche sur la nature et les technologies. A. Becker acknowledges support from the Alexander von Humboldt-Stiftung (Bonn). W. Liu (weliu@phy.ulaval.ca) is grateful for the hospitality he received at the Max-Planck-Institut für Physik komplexer Systeme.

References

1. A. Braun, G. Korn, X. Liu, D. Du, J. Squier, and G. Mourou, *Opt. Lett.* **20**, 73 (1995).
2. J. Kasparian, M. Rodriguez, G. Méjean, J. Yu, E. Salmon, H. Wille, R. Bourayou, S. Frey, Y.-B. André, A. Mysyrowicz, R. Sauerbrey, J.-P. Wolf, and L. Wöste, *Science* **301**, 61 (2003).
3. S. L. Chin and K. Miyazaki, *Jpn. J. Appl. Phys., Part 1* **38**, 2011 (1999).
4. R. Ackermann, K. Stelmazczyk, P. Rohwetter, G. Mejean, E. Salmon, J. Yu, J. Kasparian, G. Mechain, V. Bergmann, S. Schaper, B. Weise, T. Kumm, K. Rethmeier, W. Kalkner, L. Wöste, and J. P. Wolf, *Appl. Phys. Lett.* **85**, 5781 (2004).
5. E. T. J. Nibbering, P. F. Curley, G. Grillon, B. S. Prade, M. A. Franco, F. Salin, and A. Mysyrowicz, *Opt. Lett.* **21**, 62 (1996).
6. A. Brodeur, C. Y. Chien, F. A. Ilkov, S. L. Chin, O. G. Kosareva, and V. P. Kandidov, *Opt. Lett.* **22**, 304 (1997).
7. M. Mlejnek, E. M. Wright, and J. V. Moloney, *Opt. Lett.* **23**, 382 (1998).
8. A. Dubietis, E. Gaižauskas, G. Tamošauskas, and P. D. Trapani, *Phys. Rev. Lett.* **92**, 253903 (2004).
9. W. Liu, J.-F. Gravel, F. Théberge, A. Becker, and S. L. Chin, *Appl. Phys. B* **80**, 857 (2005).
10. F. Courvoisier, V. Boutou, J. Kasparian, E. Salmon, G. Méjean, J. Yu, and J.-P. Wolf, *Appl. Phys. Lett.* **83**, 123 (2003).
11. M. Kolesik and J. V. Moloney, *Opt. Lett.* **29**, 590 (2004).
12. S. Skupin, L. Bergé, U. Peschel, and F. Lederer, *Phys. Rev. Lett.* **93**, 023901 (2004).
13. E. Arevalo and A. Becker, "Variational analysis of self-focusing of intense ultrashort laser pulses in air," *Phys. Rev. E* (to be published).
14. V. P. Kandidov, O. G. Kosareva, I. S. Golubtsov, W. Liu, A. Becker, N. Aközbebek, C. M. Bowden, and S. L. Chin, *Appl. Phys. B* **77**, 149 (2003).
15. A. Talebpour, M. Abdel-Fattah, and S. L. Chin, *Opt. Commun.* **183**, 479 (2000).
16. S. A. Hosseini, Q. Luo, B. Ferland, W. Liu, N. Aközbebek, G. Roy, and S. L. Chin, *Appl. Phys. B* **77**, 697 (2003).